JOURNAL OF CHEMICAL & ENGINEERING DATA

Article

pubs.acs.org/jced

Solute Partitioning Between 1-*n*-Butyl-3-methylimidazolium Trifluoromethanesulfonate Ionic Liquid and Supercritical CO_2

Josef Planeta, Pavel Karásek, and Michal Roth*

Institute of Analytical Chemistry of the ASCR, v. v. i., Veveří 97, 60200 Brno, Czech Republic

Supporting Information

ABSTRACT: Limiting partition coefficients (*K*-factors) of a selection of low-to-medium volatility solutes in biphasic 1-*n*-butyl-3-methylimidazolium trifluoromethanesulfonate ([bmim][TfO]) ionic liquid−supercritical carbon dioxide (IL−$scCO_2$) system were obtained by capillary column supercritical fluid chromatography (SFC) with [bmim][TfO] as the stationary liquid and $scCO_2$ as the carrier fluid. Solute selection included 24 compounds of diverse volatilities and chemical functionalities and the retention factors were measured within (313.2 to 353.2) K and (7.3 to 23.2) MPa. At a constant temperature, some pressure-tunable selectivity can be obtained through changes in the operating pressure and the $scCO_2$ density. At a fixed temperature and density of CO_2, solute partition coefficients were correlated in terms of Abraham's linear solvation energy relationships. Compared to our previous studies with other ILs ([hmim][Tf_2N], [bmim][$MeSO_4$], and [thtdp][Cl]), the loss of [bmim][TfO] from the column during the experimental run was markedly lower in the present work.

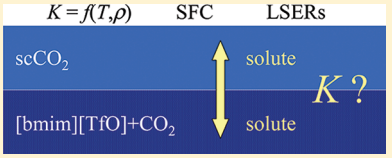

INTRODUCTION

Organic salts with melting points below 373 K, or ionic liquids (ILs), have already seen a multitude of applications in diverse fields of science and technology.[1,2] The steady growth in applications of ILs is partly tied to their extremely low vapor pressures[3,4] reflecting a significant contribution of electrostatic interactions to the cohesive energies of ILs.[5] A specific position among the uses of ILs belongs to applications combining ILs with supercritical fluids, notably supercritical carbon dioxide ($scCO_2$).[6−9] In wide regions of temperature and pressure, most ILs are not soluble in CO_2 to any measurable extent although, in turn, most ILs can absorb large amounts of CO_2.[10,11] Therefore, most IL + $scCO_2$ systems are biphasic, with their solvent properties tunable in multiple ways: by selecting from a vast portfolio of IL cations and anions as well as by adjusting the solvent power of $scCO_2$ through changes in the operating temperature and pressure. Since $scCO_2$ does not dissolve most ILs, it can be employed to extract organic nonelectrolytes from IL media,[12−16] and IL + $scCO_2$ systems have been widely used in biphasic catalysis as $scCO_2$ can serve to carry both the substrate in and the product out of the IL phase.[14,17−20] The growing applications of ILs and $scCO_2$ in phase transfer catalysis and extractions require a detailed knowledge of the underlying phase behavior,[21−24] and numerous studies have appeared of ternary IL + $scCO_2$ + organic systems with both volatile[25−29] and nonvolatile[30−34] organics at finite concentrations of all components. Conversely, the limiting (infinite-dilution) partition coefficients of organic compounds in biphasic IL + $scCO_2$ systems have been measured by supercritical fluid chromatography (SFC)[35−42] and by IR spectroscopy.[43]

To date, the development of thermodynamic models to correlate and predict limiting partition coefficients of solutes in IL + $scCO_2$ systems has largely followed two routes, one involving linear solvation energy relationships (LSERs)[36,38,40] and another using the Sanchez−Lacombe mean-field lattice gas model.[39,41] Further development of either route requires new experimental data on partition coefficients. The aim of the present contribution was to study solute partitioning in an IL + $scCO_2$ system with the IL anion derived from a very strong acid so that the effect of the anion selection on the resultant LSER parameters could be evaluated. The IL selected for the purpose was 1-*n*-butyl-3-methylimidazolium trifluoromethanesulfonate ([bmim][TfO]). To date, no partitioning data have appeared for low-volatile organics in a biphasic system composed of a TfO-containing IL and $scCO_2$.

EXPERIMENTAL SECTION

Materials. Acetophenone (CAS No. 98-86-2), aniline (CAS No. 62-53-3), anisole (methoxybenzene, CAS No. 100-66-3), azulene (bicyclo[5.3.0]decapentaene, CAS No. 275-51-4), benzil (1,2-diphenylethane-1,2-dione, CAS No. 134-81-6), benzoic acid (CAS No. 65-85-0), benzothiazole (CAS No. 95-16-9), (±)-camphor (1,7,7-trimethylbicyclo[2.2.1]heptan-2-one, CAS No. 76-22-2), coumarin (1-benzopyran-2-one, CAS No. 91-64-5), *p*-cresol (4-methylphenol, CAS No. 106-44-5), dibenzothiophene (CAS No. 132-65-0), *N*,*N*-dimethylaniline (CAS No. 121-69-7), 1-hexanol (CAS No. 111-27-3), indole (benzo[*b*]pyrrole, CAS No. 120-72-9), *α*-ionone [4-(2,6,6-trimethyl-2-cyclohexen-1-yl)-3-buten-2-one, CAS No. 127-41-3], *N*-methylaniline (CAS No. 100-61-8), naphthalene (CAS No. 91-20-3), 1-phenylethanol (CAS No. 98-85-1), 2-phenylethanol (CAS No. 60-12-8), phenol (CAS No. 108-95-2), phenoxathiin (CAS No. 262-20-4), pyrene (CAS No. 129-00-

Received: September 20, 2011
Accepted: February 28, 2012
Published: March 8, 2012

   dx.doi.org/10.1021/je200986x | *J. Chem. Eng. Data* 2012, 57, 1064−1071

0), thianaphthene (benzo[*b*]thiophene, CAS No. 95-15-8), thianthrene (CAS No. 92-85-3), and veratrole (1,2-dimethoxybenzene, CAS No. 91-16-7) were purchased from Sigma-Aldrich (Prague, Czech Republic) in the highest purity available (mole fraction purity $x \geq 0.98$) and used as received. SFC-grade CO_2 (mole fraction of residual water $<5 \times 10^{-6}$) was supplied by SIAD (Braňany u Mostu, Czech Republic). HPLC grade solvents, *n*-hexane ($x > 0.95$), methanol ($x > 0.999$), and methylene chloride ($x = 0.999$) were purchased from Sigma-Aldrich. Ionic liquid [bmim][TfO] ($x = 0.99$) was supplied by Alfa Aesar (Karlsruhe, Germany). To remove moisture and possible residual volatile impurities from [bmim][TfO] prior to the column preparation, 1 mL of [bmim][TfO] was purged with a gentle stream of nitrogen in a gas chromatographic oven at a programmed temperature, with the final period of 12 h at 403 K. Fused-silica capillary tubing for preparation of the column (100 μm i.d.) and the outlet restrictor was purchased from Agilent Technologies (Waldbronn, Germany). The reagents for surface treatment of the fused silica tubing, ammonium hydrogen difluoride and 2-chloro-1,1,2-trifluoroethylmethylether, were supplied by Sigma-Aldrich and by Apollo Scientific Ltd. (Stockport, Cheshire, U.K.), respectively.

Open-Tubular Capillary Column. To improve the adhesion of [bmim][TfO], the inner surface of fused-silica tubing was chemically treated to make it less smooth prior to the column preparation. In the first step, one-third of the tubing length was filled with liquid 2-chloro-1,1,2-trifluoroethylmethylether, both ends of the tubing were sealed by melting with a micro flame torch, and the tubing was placed in a gas chromatographic oven at 593 K for 12 h. After cooling to room temperature and flushing with methanol, the tubing was filled with saturated methanolic solution of ammonium hydrogen difluoride and etched at 313 K for 12 h. In the next step, the tubing was filled with a coating solution (74.01 mg of [bmim][TfO] in 10 mL of CH_2Cl_2), one end of the tubing was tightly sealed, and methylene chloride was carefully evaporated by applying vacuum to the open end. The resultant column was 3.325 m long, had a 100 μm i.d., and contained 6.56×10^{-7} mol [bmim][TfO]. The equivalent film thickness of [bmim][TfO] on the column inner wall at 298 K and at ambient pressure was 0.14 μm.

Apparatus and Procedure. The apparatus used in this study was a modified Varian 3700 gas chromatograph described before,[35] and the procedure was similar to that used in our previous SFC studies with other ILs.[37,38] Solute retention factors were measured along three isotherms (313, 333, and 353) K at mean column pressures within (7.3 to 23.2) MPa, with methane serving to mark the column holdup time. The pressure drop along the open tubular column was calculated from the Hagen−Poiseuille equation using the correlation for viscosity of CO_2 developed by Vesovic et al.,[44] and it did not exceed 0.016 MPa. Depending on the operating temperature and pressure, the column holdup time ranged within (240 to 660) s, the solute retention time ranged within (360 to 6120) s, and the CO_2 mass flow rate through the column ranged within (1.3×10^{-5} to 5.6×10^{-5}) g·s^{-1}. The density of CO_2 was obtained from the Span−Wagner equation of state.[45,46] To maximize the usable lifetime of the column, retention measurements were performed in the sequence of increasing density of CO_2. The 24 solutes had to be divided among 10 different injection solutions to secure well resolved peaks at all densities of CO_2. The injection solvent was *n*-hexane and the concentrations of individual solutes ranged within 1.5−3.3 mg/mL, with each injection solution containing naphthalene as a reference. Throughout the measurement procedure, the current amount of [bmim][TfO] in the column was frequently determined from regular checks of the retention factor of naphthalene at 333 K and 10 MPa as described before.[37] All retention factors were corrected to the initial amount of [bmim][TfO] in the column. At the end of the whole series of measurements, the column only contained 92.9% of the initial amount of [bmim][TfO]. The retention factors used to obtain the partition coefficients were averages of three consecutive determinations, with the relative standard deviation ranging within 2% of the mean value. Considering the standard uncertainties[47] in the measurements of the column temperature and the column inlet pressure, ± 0.15 K and ± 0.05 MPa, respectively, we estimate that the relative expanded uncertainty[47] in the resultant retention factors was ± 10%.

RESULTS AND DISCUSSION

In the following discussion, the solute will be identified by subscript 1, the principal component of the stationary (liquid) phase (= [bmim][TfO]) by subscript 2, and the carrier fluid (= CO_2) by subscript 3. Subscripts L and G will denote the quantities pertaining to the stationary and the mobile phases, respectively.

Partition Coefficients. The partition coefficients were obtained from experimental data on solute retention factor

$$k_1 = (t_R - t_0)/t_0 \quad (1)$$

where t_R is the solute retention time and t_0 the column holdup time. Depending on the intended usage and custom practices in different disciplines, several quantities are employed to describe interphase partitioning. A rigorous thermodynamic description of equilibrium distribution of the solute between both phases is provided by the *K*-factor defined as

$$K = x_{1G}/x_{1L} \quad (2)$$

where x_{1G} and x_{1L} are the equilibrium mole fractions of the solute in the gas (mobile) and liquid (stationary) phases, respectively. Under the conditions of linear chromatography,[48] the relationship between k_1 and K is

$$K = M_3 n_{2L}/[k_1 V_G \rho_{3G}(1 - x_{3L})] \quad (3)$$

where M_3 is the molar mass of CO_2, n_{2L} is the number of moles of [bmim][TfO] in the column, V_G is the void volume of the column, ρ_{3G} is the density of CO_2 at the temperature and mean pressure in the column, and $x_{3\,L}$ is the mole fraction solubility of CO_2 in [bmim][TfO].

For practical purposes in the design of processes employing IL−scCO_2 biphasic systems, the distribution of a trace amount of solute between the liquid phase containing the m_{2L} mass of the IL and the gas phase containing the m_{3G} mass of CO_2 can be described by a partition coefficient defined as[37]

$$K_N = (m_{1G}/m_{1L})(m_{2L}/m_{3G}) \quad (4)$$

where m_{1G} and $m_{1\,L}$ are the masses of the solute in the mobile and the stationary phases, respectively, at equilibrium. Under the conditions of linear chromatography,[48] K_N is related to the solute retention factor k_1 by

$$K_N = m_{2L}/(k_1 m_{3G}) \quad (5)$$

dx.doi.org/10.1021/je200986x | *J. Chem. Eng. Data* 2012, 57, 1064−1071

Table 1. Infinite-Dilution Solute *K*-Factors in [bmim][TfO]−scCO$_2$ System as Functions of Temperature *T*, Pressure *P*, and CO$_2$ Density ρ_{3G}

T = 313.2 K							
P/MPa	7.3	8.1	8.5	8.8	9.2	10.5	13.2
ρ_{3G}/kg·m^{-3}	217.0	289.8	353.9	429.1	532.0	660.1	747.4
solute							
1-hexanol	0.00681	0.0132	0.0262	0.0351	0.0508	0.0717	0.0888
1-phenylethanol			0.00365	0.00555	0.00907	0.0144	0.0216
2-phenylethanol			0.00241	0.00377	0.00631	0.0104	0.0163
acetophenone	0.00306	0.00694	0.0161	0.0234	0.0380	0.0587	0.0783
α-ionone	0.00369	0.0110	0.0318	0.0467	0.0849	0.135	
aniline					0.00469	0.00701	0.0101
anisole	0.0131	0.0244	0.0465	0.0607	0.0859		
azulene	0.00106	0.00249	0.00604	0.00918	0.0154	0.0247	0.0367
benzil					0.00536	0.00972	0.0200
benzothiazole	0.00119	0.00288	0.00711	0.0108	0.0181	0.0295	0.0444
camphor	0.00830	0.0196	0.0453	0.0645	0.0985	0.156	
coumarine					0.00394	0.00716	0.0121
dibenzothiophene			0.00173	0.00304	0.00573	0.0103	0.0189
N,*N*-dimethylaniline	0.00415	0.00985	0.0223	0.0286	0.0444	0.0639	0.0897
naphthalene	0.00270	0.00594	0.0134	0.0195	0.0308	0.0469	0.0655
N-methylaniline		0.00226	0.00490	0.00669	0.0105	0.0160	0.0242
p-cresol						0.000585	0.00222
phenoxathiin			0.00265	0.00438	0.00870	0.0164	0.0293
pyrene					0.00141	0.00315	0.00634
thianaphthene	0.00208	0.00460	0.0104	0.0153	0.0245	0.0380	0.0541
thianthrene					0.00438	0.00760	0.0155
veratrole	0.00185	0.00446	0.0108	0.0164	0.0272	0.0425	
T = 333.2 K							
P/MPa	8.7	10	10.9	12.1	13.3	16.7	
ρ_{3G}/kg·m^{-3}	221.3	290.0	350.4	442.0	523.8	657.0	
Solute							
1-hexanol	0.0118	0.0194	0.0306	0.0466	0.0624	0.0850	
1-phenylethanol			0.00425	0.00760	0.0117	0.0208	
2-phenylethanol			0.00275	0.00509	0.00808	0.0153	
acetophenone	0.00461	0.00876	0.0155	0.0275	0.0406	0.0671	
α-ionone	0.00581	0.0149	0.0302	0.0624	0.0965		
aniline			0.00271	0.00439	0.00651	0.0114	
anisole	0.0194	0.0324	0.0480	0.0708	0.0913		
azulene	0.00173	0.00358	0.00623	0.0115	0.0178	0.0324	
benzil			0.00119	0.00310	0.00624	0.0159	
benzothiazole	0.00187	0.00379	0.00690	0.0128	0.0201	0.0366	
camphor	0.0122	0.0245	0.0423	0.0718	0.100	0.147	
coumarine			0.00111	0.00242	0.00434	0.00967	
dibenzothiophene			0.00176	0.00391	0.00710	0.0160	
indole				0.000480	0.000772	0.00151	
N,*N*-dimethylaniline	0.00775	0.0145	0.0239	0.0380	0.0512	0.0815	
naphthalene	0.00430	0.00828	0.0138	0.0238	0.0351	0.0575	
N-methylaniline	0.00180	0.00342	0.00567	0.00940	0.0137	0.0239	
p-cresol			0.000525	0.000936	0.00139	0.00251	
phenol				0.000790	0.00117	0.00202	
phenoxathiin			0.00259	0.00586	0.0107	0.0242	
pyrene			0.000436	0.00108	0.00214	0.00547	
thianaphthene	0.00335	0.00619	0.0108	0.0189	0.0280	0.0479	
thianthrene			0.00122	0.00293	0.00564	0.0140	
veratrole	0.00310	0.00646	0.0113	0.0205	0.0310		
T = 353.2 K[a]							
P/MPa	10.0	11.8	13.3	15.3	17.6	23.2	
ρ_{3G}/kg·m^{-3}	221.6	288.6	352.4	439.9	526.3	658.3	
Solute							
1-hexanol	0.0115	0.0171	0.0214	0.0290	0.0356	0.0395	

dx.doi.org/10.1021/je200986x | J. Chem. Eng. Data 2012, 57, 1064−1071

Table 1. continued

T = 353.2 K[a]						
P/MPa	10.0	11.8	13.3	15.3	17.6	23.2
ρ_{3G}/kg·m^{-3}	221.6	288.6	352.4	439.9	526.3	658.3
1-phenylethanol	0.00137	0.00236	0.00341	0.00541	0.00806	0.0122
2-phenylethanol	0.000827	0.00148	0.00220	0.00366	0.00564	0.00913
acetophenone	0.00422	0.00724	0.0104	0.0156	0.0217	0.0307
α-ionone	0.00584	0.0125	0.0204	0.0349	0.0515	
aniline		0.00160	0.00211	0.00307	0.00450	0.00651
anisole	0.0170	0.0246	0.0308	0.0403	0.0478	
azulene	0.00174	0.00308	0.00456	0.00751	0.0109	0.0167
benzil		0.000476	0.000921	0.00209	0.00415	0.00921
benzothiazole	0.00183	0.00328	0.00488	0.00796	0.0120	0.0186
camphor	0.0109	0.0188	0.0268	0.0393	0.0496	
coumarine			0.000836	0.00159	0.00280	0.00561
dibenzothiophene		0.000791	0.00137	0.00268	0.00473	0.00955
indole				0.000379	0.000578	0.00106
N,*N*-dimethylaniline	0.00726	0.0110	0.0152	0.0211	0.0282	0.0363
naphthalene	0.00413	0.00692	0.00973	0.0147	0.0203	0.0274
N-methylaniline	0.00192	0.00302	0.00423	0.00627	0.00893	0.0136
p-cresol			0.000479	0.000765	0.00111	0.00181
phenol				0.000654	0.000933	0.00143
phenoxathiin	0.000485	0.00113	0.00197	0.00395	0.00702	0.0136
pyrene			0.000360	0.000801	0.00154	0.00366
thianaphthene	0.00326	0.00548	0.00776	0.0116	0.0167	0.0241
thianthrene			0.000969	0.00207	0.00394	0.00867
veratrole	0.00321	0.00568	0.00834	0.0137	0.0195	0.0268

[a]As no $x_{3\,L}$ and v_L data for the [bmim][TfO]−scCO$_2$ system at 353.2 K were available, the K-factors at 353.2 K were calculated on a CO$_2$-free-[bmim][TfO] basis, i.e., assuming x_{3L} = 0 and v_L = molar volume of pure [bmim][TfO] at the particular T and P.

In analytical chemistry, solute partition coefficient is usually defined by

$$K_c = c_{1L}/c_{1G} \quad (6)$$

where $c_{1\,L}$ and c_{1G} are the molar concentrations of the solute in the stationary and mobile phases, respectively. The quantities k_1 and K_c are related by

$$K_c = k_1 V_G(1 - x_{3L})/(n_{2L} v_L) \quad (7)$$

where v_L is the molar volume of CO$_2$-saturated [bmim][TfO].

The values of x_{3L} to be used to convert the retention factors into K or K_c via eq 3 or eq 7, respectively, were interpolated from the results of Liu et al.[34] Molar volume data from the same source on the liquid phase of the [bmim][TfO]+CO$_2$ binary system were employed to interpolate the v_L values needed in eq 7, and also to describe the variations of V_G with temperature and pressure as needed in eq 3. The values of V_G were obtained by subtracting the volume of the current amount of CO$_2$-saturated [bmim][TfO] from the geometric volume of the fused silica capillary used to prepare the column. As the composition and volumetric data on the [bmim][TfO] + CO$_2$ binary system were not available at 353.2 K, the partitioning characteristics at that temperature are estimates obtained assuming x_{3L} = 0 and v_L equal to the molar volume of pure [bmim][TfO].[49]

The resultant K-factors are listed in Table 1, and the partition coefficients K_N and K_c are compiled in the Supporting Information (Tables S1 and S2, respectively). As one can expect, neither of the three quantities K, K_N and K_c shows any definite trend with the molar mass of the solute (Table S3) although the distribution of the heaviest solutes (thianthrene, benzil, pyrene, and phenoxathiin) is shifted toward the IL phase.

LSER Fits of Relative Retention Factors. The general solvation parameter model of Abraham[50] is an efficient tool to analyze or predict free energies of partition in biphasic systems including IL−gas systems[51−53] as well as in chromatography.[51,53−55] Linear solvation energy relationships (LSERs) use only pure-component descriptors without introducing any binary interaction parameters. This provides LSERs with significant predictive power. However, when used to correlate retention data from SFC with IL stationary liquids,[36,38,40] LSERs have been applied at a fixed temperature (T) and pressure (P) as they cannot directly accommodate the composition variations in the IL+CO$_2$ mixture that follow from the changes in the two operating parameters. Recently, Machida et al.[39,41] modeled SFC retention factors in IL−CO$_2$ systems with Sanchez−Lacombe equation of state (S−L EoS).[56,57] In a particular solute−IL−CO$_2$ system, the S−L EoS proved to be very flexible and accurate in describing variations of solute retention factor with temperature and pressure. The flexibility and accuracy resulted from introducing unlike binary interaction parameters that had to be adjusted by fitting the experimental data; therefore, predictive ability of S−L EoS for other solutes is somewhat limited as compared to that of LSERs.

The solute molecular descriptors used in the present study were those tabulated by Abraham et al.[58] To minimize the uncertainty coming from the determination of the mass of [bmim][TfO] in the column, the regressed quantity was the retention factor of the particular solute A expressed relatively to the retention factor of a reference solute (B = naphthalene) at the particular temperature and pressure, k_A/k_B. It follows from

dx.doi.org/10.1021/je200986x | J. Chem. Eng. Data 2012, 57, 1064−1071

eqs 3, 5 and 7 that the relative retention factor equals the relative partition coefficient, $k_A/k_B = K_B/K_A = K_{NB}/K_{NA} = K_{cA}/K_{cB}$. Linear regression of relative retention factors at 353.2 K and 17.6 MPa on the solute molecular descriptors yields

$$\log(k_A/k_B) = 0.993E_A + 0.364S_A + 2.343A_A + 0.311B_A - 1.500V_A \quad (8)$$

where the solute dimensionless descriptors[58,59] E_A, S_A, A_A, B_A, and V_A of solute A describe the solute's excess molar refractivity, dipolarity/polarizability, hydrogen bond acidity (= hydrogen bond donating ability), hydrogen bond basicity (= hydrogen bond accepting ability), and the solute molecular size proportional to the McGowan's characteristic volume of the solute,[60] respectively. Figure 1 shows a comparison of experimental values of k_A/k_B with those calculated from eq 8.

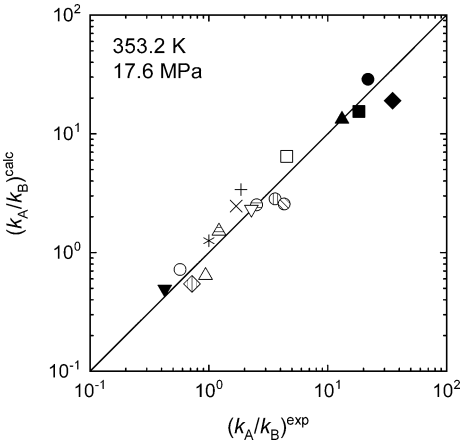

Figure 1. LSER fit of relative retention factors. ○, 1-hexanol; horizontally hatched ○, 1-phenylethanol; vertically hatched ○, 2-phenylethanol; △, acetophenone; □, aniline; ▼, anisole; +, azulene; ×, benzothiazole; diagonally hatched ○, dibenzothiophene; ♦, indole; vertically hatched ◊, *N*,*N*-dimethylaniline; *, naphthalene; ▽ *N*-methylaniline; ■, *p*-cresol; ●, phenol; ▲, pyrene; horizontally hatched Δ, thianaphthene.

At 353.2 K and 15.3 MPa, with the same solute set as that shown in Figure 1, the LSER fit is

$$\log(k_A/k_B) = 1.156E_A + 0.291S_A + 2.404A_A + 0.442B_A - 1.640V_A \quad (9)$$

and at 333.2 K and 13.3 MPa, again with the same set of solutes

$$\log(k_A/k_B) = 1.136E_A + 0.305S_A + 2.616A_A + 0.418B_A - 1.641V_A \quad (10)$$

The magnitudes of numerical coefficients in eqs 8−10 can be viewed as sensitivities of solute partition coefficients to the property described by the particular descriptor. In this context, it is useful to compare the present LSERs in [bmim][TfO]−scCO$_2$ system with previous results in 1-*n*-butyl-3-methylimidazolium tetrafluoroborate ([bmim][BF$_4$])-, trihexyltetradecylphosphonium chloride ([thtdp][Cl])-, and 1-*n*-butyl-3-methylimidazolium methyl sulfate ([bmim][MeSO$_4$])-containing systems.[36,38,40] Sensitivities of k_A/k_B to the particular properties of solute A vary among the individual IL−scCO$_2$ systems as follows:

Solute excess molar refractivity: [thtdp][Cl] > [bmim][MeSO$_4$] ≈ [bmim][BF$_4$] ≈ [bmim][TfO].
Solute dipolarity/polarizability: [thtdp][Cl] > [bmim][TfO] > [bmim][MeSO$_4$] ≈ [bmim][BF$_4$].
Solute H-bond acidity: [thtdp][Cl] > [bmim][MeSO$_4$] > [bmim][BF$_4$] > [bmim][TfO].
Solute H-bond basicity: [thtdp][Cl] > [bmim][MeSO$_4$] > [bmim][BF$_4$] > [bmim][TfO].
Solute molecular volume: [bmim][MeSO$_4$] > [bmim][BF$_4$] > [bmim][TfO] > [thtdp][Cl].

In the above comparisons, the phosphonium-based IL, [thtdp][Cl], always takes an outlying position. Therefore, although the solute sets used to obtain the LSERs differed somewhat among the individual IL−scCO$_2$ systems,[36,38,40] the above relations confirm the earlier finding[40] that the sensitivities observed with [thtdp][Cl] stand apart those of imidazolium-based ILs suggesting that the effect of IL cation on k_A/k_B exceeds the effect of IL anion. As regards the effects of anions in the family of imidazolium ILs involved, it appears that the sensitivities of k_A/k_B reach their limiting values with [bmim][TfO]. The low sensitivity of k_A/k_B in [bmim][TfO]−CO$_2$ system to the solute acidity and basicity descriptors may possibly reflect the very strong acidity of trifluoromethanesulfonic acid. The sensitivities of k_A/k_B to the solute excess molar refractivity and molecular volume descriptors are also low in the [bmim][TfO]−CO$_2$ system although the reason is not apparent here. Overall, with the particular selection of imidazolium and phosphonium ILs, the sensitivities may reflect the structural differences; in [thtdp][Cl], the charges of both cation and anion are pinpointed to a single atom whereas in imidazolium-based ILs the charges are delocalized.

Variation of Retention Factors with CO$_2$ Density. At a constant temperature, the retention factor of a solute in SFC decreases with increasing density, ρ_{3G}, of CO$_2$, and the plots of ln k_1 vs ln ρ_{3G} are often nearly linear,[61] with the slope given by[62]

$$\left(\frac{\partial \ln k_1}{\partial \ln \rho_{3G}}\right)_T = \frac{1}{RT\beta_{3T}}\left[\bar{V}_{1G}^{\infty} - \bar{V}_{1L}^{\infty} - \left(\frac{\partial \mu_{1L}^{\infty}}{\partial x_{3L}}\right)_{T,P,n_{2L}} \left(\frac{\partial x_{3L}}{\partial P}\right)_{T,\sigma}\right] - \frac{V_L}{V_G}\frac{\beta_{LT\sigma}}{\beta_{3T}} \quad (11)$$

where R is the molar gas constant, T is the temperature, P is the pressure, V_L is the volume of the CO$_2$-saturated [bmim][TfO] in the column, β_{3T} is the isothermal compressibility of CO$_2$, $\beta_{LT\sigma}$ is the isothermal compressibility of CO$_2$-saturated [bmim][TfO], μ_{1L}^{∞} is the infinite-dilution chemical potential of the solute in CO$_2$-saturated [bmim][TfO], and $\bar{V}_{1G}^{\infty}$ and $\bar{V}_{1L}^{\infty}$ are the infinite-dilution partial molar volumes of the solute in CO$_2$ and in CO$_2$-saturated [bmim][TfO], respectively. Figure 2 shows an example of the ln k_1 vs ln ρ_{3G} plot, and numerical values of the slopes $(\partial \ln k_1/\partial \ln \rho_{3G})_T$ in all solutes and retention isotherms are compiled in the Supporting Information (Table S4). At a constant temperature, there is an approximate correlation between the slope $(\partial \ln k_1/\partial \ln \rho_{3G})_T$ and the solute molecular size. Figure 3 illustrates such a correlation at 333 K, with the solute molecular size measured by the McGowan's characteristic volume.[60] The McGowan's volumes of individual solutes were calculated using the group contribution model and spreadsheet calculator developed by

dx.doi.org/10.1021/je200986x | J. Chem. Eng. Data 2012, 57, 1064−1071

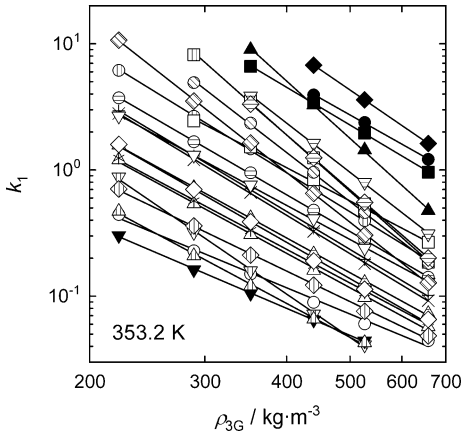

Figure 2. Retention factors vs CO_2 density at 353.2 K. ○, 1-hexanol; horizontally hatched ○, 1-phenylethanol; vertically hatched ○, 2-phenylethanol; △, acetophenone; vertically hatched ▽, α-ionone; □, aniline; ▼, anisole; +, azulene; vertically hatched □, benzil; × , benzothiazole; vertically hatched △, camphor; horizontally hatched ▽, coumarin; diagonally hatched ○, dibenzothiophene; ♦, indole; vertically hatched ◊, *N*,*N*-dimethylaniline; *, naphthalene; ▽, *N*-methylaniline; ■, *p*-cresol; ●, phenol; diagonally hatched ◊, phenoxathiin; ▲, pyrene; horizontally hatched Δ, thianaphthene; horizontally hatched ◊, thianthrene; ◊, veratrole.

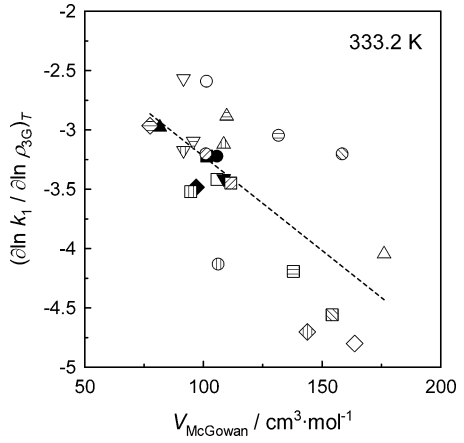

Figure 3. Approximate correlation between $(\partial \ln k_1/\partial \ln \rho_{3G})_T$ at 333.2 K and McGowan's characteristic volume of the solute. Symbol key is the same as in Figure 2.

Zhao et al.[63] It appears that, with the increasing size of the solute molecule, the slope $(\partial \ln k_1/\partial \ln \rho_{3G})_T$ tends to become more negative (i.e., larger in magnitude). This is because the most important terms on the right-hand side of eq 11 are those with $\overline{V}^{\infty}_{1G}$ and $(\partial \mu^{\infty}_{1L}/\partial x_{3L})_{T,P,n_{2L}}$. Aside from reflecting the intermolecular interactions, both terms also depend on the solute molecular size, thus giving rise to the loose correlation between $(\partial \ln k_1/\partial \ln \rho_{3G})_T$ and the molecular size as shown in Figure 3. Naturally, the correlation is not strong because of the dependence of all terms in eq 11 on intermolecular interactions.

When comparing the slopes with the corresponding results obtained for other ILs before,[35−38,40] no clear-cut trend emerges. This is because in a particular solute and a particular isotherm, the different slopes $(\partial \ln k_1/\partial \ln \rho_{3G})_T$ in columns with various ILs are associated with the terms containing x_{3L}, i.e., with the pressure coefficient of CO_2 solubility in the IL, $(\partial x_{3L}/\partial P)_{T,\sigma}$, and with the sensitivity of the solute chemical potential to the composition of the IL + CO_2 stationary phase, $(\partial \mu^{\infty}_{1L}/\partial x_{3L})_{T,P,n_{2L}}$.

Column Stability. The capillary column with [bmim][TfO] proved to be significantly more stable as compared to the columns with other ILs used in the previous studies. In the present work, only about 7 % of the initial amount of [bmim][TfO] were lost from the column during the measurement series as compared to the losses of 23 % with [hmim][Tf_2N],[37] 27 % with [bmim][$MeSO_4$],[40] and 31 % with [thtdp][Cl].[38] Moreover, because of a larger number of solutes, the present measurements with [bmim][TfO] were of longer duration than the previous studies so that a larger amount of CO_2 had to pass through the present column, thus underlining the enhanced stability of the [bmim][TfO] column. The potential factors explaining this observation may include a lower solubility of [bmim][TfO] in $scCO_2$, a lower reduction of [bmim][TfO] viscosity on absorption of CO_2, and/or improved adhesion of [bmim][TfO] to the fused silica column wall as compared to the other ILs mentioned above.

CONCLUSION

The present work extends the database of infinite dilution partition coefficients of organic solutes in biphasic IL−$scCO_2$ systems by the results for [bmim][TfO]. Infinite dilution partition coefficients of 24 low-to-medium volatility solutes in biphasic [bmim][TfO]−$scCO_2$ system were obtained by SFC within (313.2 to 353.2) K and (7.3 to 23.2) MPa. At fixed temperature and pressure conditions, relative partition coefficients were correlated with the LSER relationships. The resultant LSER parameters are close to those observed before with other bmim-containing ILs while differing distinctly from those obtained with phosphonium-based IL [thtdp][Cl]. Compared to previous results with [bmim][BF_4] and [bmim][$MeSO_4$], the LSER parameters obtained with [bmim][TfO] are less sensitive to the solute hydrogen bond acidity and basicity descriptor, possibly reflecting the "superacidity" of trifluoromethanesulfonic acid.

ASSOCIATED CONTENT

Supporting Information

Solute structures and numerical data on solute partition coefficients K_N (Table S1) and K_c (Table S2) in [bmim][TfO]−$scCO_2$ system together with selected properties of the pure solutes (Table S3) and the solute retention−density slopes $(\partial \ln k_1/\partial \ln \rho_{3G})_T$ (Table S4). This material is available free of charge via the Internet at http://pubs.acs.org.

AUTHOR INFORMATION

Corresponding Author

*Phone: +420 532 290 171. Fax: +420 541 212 113. E-mail: roth@iach.cz.

Funding

We thank the Czech Science Foundation (Project No. P206/11/0138) and the Academy of Sciences of the Czech Republic (Institutional Research Plan AV0Z40310501) for financial support of this work.

Notes

The authors declare no competing financial interest.

REFERENCES

(1) Plechkova, N. V.; Seddon, K. R. Applications of ionic liquids in the chemical industry. *Chem. Soc. Rev.* **2008**, *37*, 123−150.

(2) Hallett, J. P.; Welton, T. Room-Temperature Ionic Liquids: Solvents for Synthesis and Catalysis. 2. *Chem. Rev.* **2011**, *111*, 3508−3576.
(3) Zaitsau, D. H.; Kabo, G. J.; Strechan, A. A.; Paulechka, Y. U.; Tschersich, A.; Verevkin, S. P.; Heintz, A. Experimental Vapor Pressures of 1-Alkyl-3-methylimidazolium Bis-(trifluoromethylsulfonyl)imides and a Correlation Scheme for Estimation of Vaporization Enthalpies of Ionic Liquids. *J. Phys. Chem. A* **2006**, *110*, 7303−7306.
(4) Esperança, J. M. S. S.; Canongia Lopes, J. N.; Tariq, M.; Santos, L. M. N. B. F.; Magee, J. W.; Rebelo, L. P. N. Volatility of Aprotic Ionic Liquids − A Review. *J. Chem. Eng. Data* **2010**, *55*, 3−12.
(5) Armstrong, J. P.; Hurst, C.; Jones, R. G.; Licence, P.; Lovelock, K. R. J.; Satterley, C. J.; Villar-Garcia, I. J. Vapourisation of ionic liquids. *Phys. Chem. Chem. Phys.* **2007**, *9*, 982−990.
(6) Dzyuba, S. V.; Bartsch, R. A. Recent Advances in Applications of Room-Temperature Ionic Liquid/Supercritical CO_2 Systems. *Angew. Chem., Int. Ed.* **2003**, *42*, 148−150.
(7) Keskin, S.; Kayrak-Talay, D.; Akman, U.; Hortaçsu, Ö. A review of ionic liquids towards supercritical fluid applications. *J. Supercrit. Fluids* **2007**, *43*, 150−180.
(8) Roth, M. Partitioning behaviour of organic compounds between ionic liquids and supercritical fluids. *J. Chromatogr. A* **2009**, *1216*, 1861−1880.
(9) Jutz, F.; Andanson, J.-M.; Baiker, A. Ionic Liquids and Dense Carbon Dioxide: A Beneficial Biphasic System for Catalysis. *Chem. Rev.* **2011**, *111*, 322−353.
(10) Niehaus, D.; Philips, M.; Michael, A.; Wightman, R. M. Voltammetry of ferrocene in supercritical carbon dioxide containing water and tetrahexylammonium hexafluorophosphate. *J. Phys. Chem.* **1989**, *93*, 6232−6236.
(11) Blanchard, L. A.; Gu, Z.; Brennecke, J. F. High-Pressure Phase Behavior of Ionic Liquid/CO_2 Systems. *J. Phys. Chem. B* **2001**, *105*, 2437−2444.
(12) Blanchard, L. A.; Hancu, D.; Beckman, E. J.; Brennecke, J. F. Green processing using ionic liquids and CO_2. *Nature* **1999**, *399*, 28−29.
(13) Blanchard, L. A.; Brennecke, J. F. Recovery of Organic Products from Ionic Liquids Using Supercritical Carbon Dioxide. *Ind. Eng. Chem. Res.* **2001**, *40*, 287−292.
(14) Brown, R. A.; Pollet, P.; McKoon, E.; Eckert, C. A.; Liotta, C. L.; Jessop, P. G. Asymmetric Hydrogenation and Catalyst Recycling Using Ionic Liquid and Supercritical Carbon Dioxide. *J. Am. Chem. Soc.* **2001**, *123*, 1254−1255.
(15) Bortolini, O.; Campestrini, S.; Conte, V.; Fantin, G.; Fogagnolo, M.; Maietti, S. Sustainable Epoxidation of Electron-Poor Olefins with Hydrogen Peroxide in Ionic Liquids and Recovery of the Products with Supercritical CO_2. *Eur. J. Org. Chem.* **2003**, 4804−4809.
(16) Kroon, M. C.; van Spronsen, J.; Peters, C. J.; Sheldon, R. A.; Witkamp, G.-J. Recovery of pure products from ionic liquids using supercritical carbon dioxide as a co-solvent in extractions or as an anti-solvent in precipitations. *Green Chem.* **2006**, *8*, 246−249.
(17) Liu, F.; Abrams, M. B.; Baker, R. T.; Tumas, W. Phase-separable catalysis using room temperature ionic liquids and supercritical carbon dioxide. *Chem. Commun.* **2001**, 433−434.
(18) Sellin, M. F.; Webb, P. B.; Cole-Hamilton, D. J. Continuous flow homogeneous catalysis: hydroformylation of alkenes in supercritical fluid−ionic liquid biphasic mixtures. *Chem. Commun.* **2001**, 781−782.
(19) Bösmann, A.; Franciò, G.; Janssen, E.; Solinas, M.; Leitner, W.; Wasserscheid, P. Activation, Tuning, and Immobilization of Homogeneous Catalysts in an Ionic Liquid/Compressed CO_2 Continuous-Flow System. *Angew. Chem., Int. Ed.* **2001**, *40*, 2697−2699.
(20) Lozano, P.; de Diego, T.; Carrié, D.; Vaultier, M.; Iborra, J. L. Continuous green biocatalytic processes using ionic liquids and supercritical carbon dioxide. *Chem. Commun.* **2002**, 692−693.
(21) Kühne, E.; Martin, A.; Witkamp, G.-J.; Peters, C. J. Modeling the Phase Behavior of Ternary Systems Ionic Liquid + Organic + CO_2 with a Group Contribution Equation of State. *AIChE J.* **2009**, *55*, 1265−1273.
(22) Raeissi, S.; Florusse, L.; Peters, C. J. Scott−van Konynenburg phase diagram of carbon dioxide + alkylimidazolium-based ionic liquids. *J. Supercrit. Fluids* **2010**, *55*, 825−832.
(23) Smith, R. L.; Fang, Z. Properties and phase equilibria of fluid mixtures as the basis for developing green chemical processes. *Fluid Phase Equilib.* **2011**, *302*, 65−73.
(24) Kroon, M. C.; Florusse, L. J.; Kühne, E.; Witkamp, G.-J.; Peters, C. J. Achievement of a Homogeneous Phase in Ternary Ionic Liquid/Carbon Dioxide/Organic Systems. *Ind. Eng. Chem. Res.* **2010**, *49*, 3474−3478.
(25) Scurto, A. M.; Aki, S. N. V. K.; Brennecke, J. F. CO_2 as a Separation Switch for Ionic Liquid/Organic Mixtures. *J. Am. Chem. Soc.* **2002**, *124*, 10276−10277.
(26) Najdanovic-Visak, V.; Serbanovic, A.; Esperança, J. M. S. S.; Guedes, H. J. R.; Rebelo, L. P. N; Nunes da Ponte, M. Supercritical Carbon Dioxide-Induced Phase Changes in (Ionic Liquid, Water and Ethanol Mixture) Solutions: Application to Biphasic Catalysis. *ChemPhysChem* **2003**, *4*, 520−522.
(27) Ahn, J.-Y.; Lee, B.-C.; Lim, J. S.; Yoo, K.-P.; Kang, J. W. High-pressure phase behavior of binary and ternary mixtures containing ionic liquid [C_6-mim][Tf_2N], dimethyl carbonate and carbon dioxide. *Fluid Phase Equilib.* **2010**, *290*, 75−79.
(28) Chobanov, K.; Tuma, D.; Maurer, G. High-pressure phase behavior of ternary systems (carbon dioxide + alkanol + hydrophobic ionic liquid). *Fluid Phase Equilib.* **2010**, *294*, 54−66.
(29) Bogel-Łukasik, R.; Matkowska, D.; Zakrzewska, M. E.; Bogel-Łukasik, E.; Hofman, T. The phase envelopes of alternative solvents (ionic liquid, CO_2) and building blocks of biomass origin (lactic acid, propionic acid). *Fluid Phase Equilib.* **2010**, *295*, 177−185.
(30) Kühne, E.; Peters, C. J.; van Spronsen, J.; Witkamp, G.-J. Solubility of carbon dioxide in systems with [bmim][BF_4] and some selected organic compounds of interest for the pharmaceutical industry. *Green Chem.* **2006**, *8*, 287−291.
(31) Fu, D. B.; Sun, X. W.; Qiu, Y. H.; Jiang, X. H.; Zhao, S. Q. High-pressure phase behavior of the ternary system CO_2 + ionic liquid [bmim][PF_6] + naphthalene. *Fluid Phase Equilib.* **2007**, *251*, 114−120.
(32) Kühne, E.; Santarossa, S.; Perez, E.; Witkamp, G. J.; Peters, C. J. New approach in the design of reactions and separations using an ionic liquid and carbon dioxide as solvents: Phase equilibria in two selected ternary systems. *J. Supercrit. Fluids* **2008**, *46*, 93−98.
(33) Bogel-Łukasik, R.; Najdanovic-Visak, V.; Barreiros, S.; Nunes da Ponte, M. Distribution Ratios of Lipase-Catalyzed Reaction Products in Ionic Liquid Supercritical CO_2 Systems: Resolution of 2-Octanol Enantiomers. *Ind. Eng. Chem. Res.* **2008**, *47*, 4473−4480.
(34) Liu, J.; Sun, X. W.; Fu, D. B.; Zhao, S. Q. Phase equilibria for separation of high boiling point organics from ionic liquids by supercritical CO_2 or C_3H_8. *Chem. Eng. J.* **2009**, *147*, 63−70.
(35) Planeta, J.; Roth, M. Partition Coefficients of Low-Volatility Solutes in the Ionic Liquid 1-*n*-Butyl-3-methylimidazolium Hexafluorophosphate−Supercritical CO_2 System from Chromatographic Retention Measurements. *J. Phys. Chem. B* **2004**, *108*, 11244−11249.
(36) Planeta, J.; Roth, M. Solute Partitioning Between the Ionic Liquid 1-*n*-Butyl-3-methylimidazolium Tetrafluoroborate and Supercritical CO_2 from Capillary-Column Chromatography. *J. Phys. Chem. B* **2005**, *109*, 15165−15171.
(37) Planeta, J.; Karásek, P.; Roth, M. Distribution of sulfur-containing aromatics between [hmim][Tf_2N] and supercritical CO_2: a case study for deep desulfurization of oil refinery streams by extraction with ionic liquids. *Green Chem.* **2006**, *8*, 70−77.
(38) Planeta, J.; Karásek, P.; Roth, M. Limiting Partition Coefficients of Solutes in Biphasic Trihexyltetradecylphosphonium Chloride Ionic Liquid−Supercritical CO_2 System: Measurement and LSER-Based Correlation. *J. Phys. Chem. B* **2007**, *111*, 7620−7625.
(39) Machida, H.; Y. Sato, Y.; Smith, R. L. Measurement and correlation of infinite dilution partition coefficients of aromatic compounds in the ionic liquid 1-butyl-3-methyl-imidazolium hexafluorophosphate ([bmim][PF_6])−CO_2 system at temperatures from

313 to 353 K and at pressures up to 16 MPa. *J. Supercrit. Fluids* **2008**, *43*, 430−437.
(40) Planeta, J.; Karásek, P.; Roth, M. Distribution of Organic Solutes in Biphasic 1-*n*-Butyl-3-methylimidazolium Methyl Sulfate−Supercritical CO_2 System. *J. Phys. Chem. B* **2009**, *113*, 9520−9526.
(41) Machida, H.; Kawasumi, T.; Endo, W.; Sato, Y.; Smith, R. L. Ionic liquid structural effects on solute partitioning in biphasic ionic liquid and supercritical carbon dioxide systems. *Fluid Phase Equilib.* **2010**, *294*, 114−120.
(42) Planeta, J.; Šťavíková, L.; Karásek, P.; Roth, M. Limiting Partition Coefficients of Sulfur-Containing Aromatics in Biphasic [bmim][$MeSO_4$]−Supercritical CO_2 System. *J. Chem. Eng. Data* **2011**, *56*, 527−531.
(43) Sakellarios, N. I.; Kazarian, S. G. Solute partitioning between an ionic liquid and high-pressure CO_2 studied with *in situ* FTIR spectroscopy. *J. Chem. Thermodyn.* **2005**, *37*, 621−626.
(44) Vesovic, V.; Wakeham, W. A.; Olchowy, G. A.; Sengers, J. V.; Watson, J. T. R.; Millat, J. The Transport Properties of Carbon Dioxide. *J. Phys. Chem. Ref. Data* **1990**, *19*, 763−808.
(45) Span, R.; Wagner, W. A New Equation of State for Carbon Dioxide Covering the Fluid Region from the Triple-Point Temperature to 1100 K at Pressures up to 800 MPa. *J. Phys. Chem. Ref. Data* **1996**, *25*, 1509−1596.
(46) Wagner, W.; Overhoff, U. *ThermoFluids. Interactive software for the calculation of thermodynamic properties for more than 60 pure substances*; Springer-Verlag: Berlin, 2006.
(47) Chirico, R. D.; Frenkel, M.; Diky, V. V.; Marsh, K. N.; Wilhoit, R. C. ThermoML − An XML-Based Approach for Storage and Exchange of Experimental and Critically Evaluated Thermophysical and Thermochemical Property Data. 2. Uncertainties. *J. Chem. Eng. Data* **2003**, *48*, 1344−1359.
(48) Giddings, J. C. *Dynamics of Chromatography. Part I. Principles and Theory*; Marcel Dekker: New York, 1965; p 8.
(49) Gardas, R. L.; Freire, M. G.; Carvalho, P. J.; Marrucho, I. M.; Fonseca, I. M. A.; Ferreira, A. G. M.; Coutinho, J. A. P. High-Pressure Densities and Derived Thermodynamic Properties of Imidazolium-Based Ionic Liquids. *J. Chem. Eng. Data* **2007**, *52*, 80−88.
(50) Abraham, M. H. Scales of solute hydrogen-bonding: their construction and application to physicochemical and biochemical processes. *Chem. Soc. Rev.* **1993**, *22*, 73−83.
(51) Poole, C. F. Chromatographic and spectroscopic methods for the determination of solvent properties of room temperature ionic liquids. *J. Chromatogr. A* **2004**, *1037*, 49−82.
(52) Abraham, M. H.; Acree, W. E. Comparative analysis of solvation and selectivity in room temperature ionic liquids using the Abraham linear free energy relationship. *Green Chem.* **2006**, *8*, 906−915.
(53) Breitbach, Z. S.; Armstrong, D. W. Characterization of phosphonium ionic liquids through a linear solvation energy relationship and their use as GLC stationary phases. *Anal. Bioanal. Chem.* **2008**, *390*, 1605−1617.
(54) Abraham, M. H.; Ibrahim, A.; Zissimos, A. M. Determination of sets of solute descriptors from chromatographic measurements. *J. Chromatogr. A* **2004**, *1037*, 29−47.
(55) Vitha, M.; Carr, P. W. The chemical interpretation and practice of linear solvation energy relationships in chromatography. *J. Chromatogr. A* **2006**, *1126*, 143−194.
(56) Sanchez, I. C.; Lacombe, R. H. An Elementary Molecular Theory of Classical Fluids. Pure Fluids. *J. Phys. Chem.* **1976**, *80*, 2352−2362.
(57) Sanchez, I. C.; Lacombe, R. H. Statistical Thermodynamics of Polymer Solutions. *Macromolecules* **1978**, *11*, 1145−1156.
(58) Abraham, M. H.; Chadha, H. S.; Whiting, G. S.; Mitchell, R. C. Hydrogen Bonding. 32. An Analysis of Water−Octanol and Water−Alkane Partitioning and the Δlog P Parameter of Seiler. *J. Pharm. Sci.* **1994**, *83*, 1085−1100.
(59) Abraham, M. H.; Benjelloun-Dakhama, N.; Gola, J. M. R.; Acree, W. E.; Cain, W. S.; Cometto-Muniz, J. E. Solvation descriptors for ferrocene, and the estimation of some physicochemical and biochemical properties. *New J. Chem.* **2000**, *24*, 825−829.
(60) Abraham, M. H.; McGowan, J. C. The use of characteristic volumes to measure cavity terms in reversed phase liquid chromatography. *Chromatographia* **1987**, *23*, 243−246.
(61) Lauer, H. H.; McManigill, D.; Board, R. D. Mobile-Phase Transport Properties of Liquefied Gases in Near-Critical and Supercritical Fluid Chromatography. *Anal. Chem.* **1983**, *55*, 1370−1375.
(62) Roth, M. Enthalpy of transfer in supercritical fluid chromatography. *J. Chromatogr. A* **1991**, *543*, 262−265.
(63) Zhao, Y. H.; Abraham, M. H.; Zissimos, A. M. Fast Calculation of van der Waals Volume as a Sum of Atomic and Bond Contributions and Its Application to Drug Compounds. *J. Org. Chem.* **2003**, *68*, 7368−7373.